HIGH-RESOLUTION SEISMIC STRATIGRAPHY OF A NARROW, BEDROCK-CONTROLLED ESTUARY: THE GUADIANA ESTUARINE SYSTEM, SW IBERIA

F.J. LOBO,[1] J.M.A. DIAS,[1] R. GONZÁLEZ,[1] F.J. HERNÁNDEZ-MOLINA,[2] J.A. MORALES,[3] AND V. DÍAZ DEL RÍO[4]
[1] *CIACOMAR/CIMA, Universidade do Algarve, Avenida 16 de Junho s/n, 8700-311 Olhão, Portugal*
e-mail: pacolobo@ualg.pt
[2] *Departamento de Geociencias Marinas y Ordenación del Territorio, Facultad de Ciencias, Universidad de Vigo, 36200 Vigo, Spain*
[3] *Departamento de Geología, Facultad de Ciencias Experimentales, Universidad de Huelva, 21819 Huelva, Spain*
[4] *Instituto Español de Oceanografía, Centro Oceanográfico de Málaga, Puerto Pesquero s/n, 29640 Fuengirola, Spain*

ABSTRACT: **The late Quaternary sedimentary architecture of the Guadiana estuary (southwestern Iberian Peninsula), a narrow, bedrock-controlled estuary with moderate sediment supply, was studied by applying concepts of high-resolution seismic stratigraphy. The estuarine sedimentary infill consists of a discontinuous basal interval overlain by five seismic units bounded by laterally continuous seismic horizons. The correlation between seismic facies and a stratigraphic section of the Guadiana valley enables the proposal of a detailed sequence stratigraphic interpretation of the estuarine infill.**

During the last glacial lowstand, the Guadiana was a subaerial valley with no significant accumulation of fluvial deposits because of increased sediment bypass towards the present-day middle and outer shelf. Towards the end of the postglacial transgression, the subaerial valley was transformed into an estuary, and sediments began preferentially accumulating in structural depressions. Furthermore, flood tidal currents constrained by basement highs enhanced sand deposition in the upper part of the estuary. Wave influence was reduced and confined to the lower estuarine system. Here, the narrow morphology of the valley led to an increased sediment export to the shelf during the Holocene highstand period.

The lower part of the estuarine infill consists of four fifth-order depositional sequences, composed of regressive deposits (HST). The last glacial maximum is recorded by a distinct stratigraphic surface, representing simultaneously the sequence boundary and the transgressive surface. A tidal ravinement surface is characterized by strong erosion and channel formation in the outer estuarine zones. The maximum flooding surface is identified by change of stratal patterns between landward-prograding transgressive deposits and downlapping highstand deposits. Both transgressive (TST) and regressive tracts (HST) were deposited during the final part of the postglacial transgression and subsequent highstand.

INTRODUCTION

In recent years, the application of sequence stratigraphic concepts has proven to be a valuable tool for determining the recent geological history of estuarine systems (e.g., Allen 1991; Dalrymple et al. 1992; Allen and Posamentier 1993; Zhang and Li 1996; Dabrio et al. 2000) and for establishing a relationship between their long-term evolution and estuarine physiography, filling history, hydrologic regime, and sea-level fluctuations (Frey and Howard 1986). Some researchers have used high-resolution (HR) seismic profiles to reconstruct the recent stratigraphy and evolution of estuarine valleys (Dalrymple and Zaitlin 1994; Larcombe and Jago 1994; Fenster and FitzGerald 1996; Lessa et al. 1998).

A typical estuarine sequence is composed, from bottom to top, of the following systems tracts (Allen and Posamentier 1993) (Fig. 1): (1) lowstand systems tract (LST), composed of fluvial sands and gravels, overlying the sequence boundary (SB), formed during sea-level lowstand by subaerial exposure and wave erosion; (2) transgressive systems tract (TST), separated from the LST by the transgressive surface and formed by estuarine sands and muds, highly influenced by tidal action. A tidal ravinement surface (TRS) is generated as tidal currents move landward (Allen 1991). Eventually, in wave-dominated estuaries the landward shoreline movement causes wave erosion of the tidal-inlet sands, producing a wave ravinement surface (WRS); (3) highstand systems tract (HST), constituted by a seaward-prograding wedge composed of estuarine point bars, tidal bars, and tidal flats downlapping onto a maximum flooding surface (MFS) that overlies the estuary-mouth sands and central-basin muds. This general scheme varies locally as a function of the specific physiography, sediment supply, and hydrology of the estuarine system. The recognition and interpretation of estuarine systems-tract boundaries, such as the SB, the TS, and the MFS, are especially controversial, inasmuch as they may be amalgamated with other stratigraphic surfaces (Zhang and Li 1996; Lessa et al. 1998).

Most previous studies of estuarine fills have been conducted in areas dominated by either tides (Allen 1990; Allen and Posamentier 1993; Dalrymple and Zaitlin 1994) or waves (Boyd and Honig 1992; Lessa et al. 1998), or in estuaries characterized by large fluvial sediment supply (Cooper 1993; Hori et al. 2001). The present study focuses on the Guadiana estuary (southwestern Iberian Peninsula), which is a bedrock-controlled, narrow, relatively straight estuary. Besides, the fluvial supply is dominated by episodic, seasonal events, in contrast to many temperate river basins. The characterization of estuarine seismic facies and their boundaries in the Guadiana estuary can provide significant information about the influence of estuarine morphology on recent hydrologic changes and the effects of late Quaternary sea-level fluctuations on the preservation potential of depositional sequences, as seen in the Gulf of Cadiz coastal (Zazo et al. 1994; Zazo et al. 1996; Goy et al. 1996) and shelf (Somoza et al. 1997; Hernández-Molina et al. 2000) sedimentary record. In this sense, the main goals of the present work are: (1) analysis of the seismic stratigraphic architecture of the estuarine sedimentary fill; (2) definition of the neotectonic control on the estuarine valley and of estuary-to-shelf sediment transfer; (3) correlation between seismic facies and estuarine margin deposits; and (4) elaboration of a late Quaternary seismic-sequence stratigraphic model.

MORPHOLOGY, HYDROLOGY, AND STRATIGRAPHY OF THE GUADIANA RIVER ESTUARY

Estuary Morphology

The Guadiana river is 730 km long. Its estuary is located at the southwest corner of the Iberian Peninsula, forming the border between Spain and Portugal (Fig. 2). Two different physiographic domains characterize the Guadiana estuary (Morales 1997): (1) The estuary *sensu stricto* or estuarine valley, characterized by complex interactions between fluvial and marine processes; (2) A prograding complex, formed by sandy areas and marshes in the littoral plain (González et al. 2001) (Fig. 2).

The Guadiana estuarine valley is cut into Paleozoic bedrock, composed mainly of a thick succession of highly deformed Paleozoic turbidites. Only the outermost 5 km are underlain by Cretaceous and Jurassic limestones. The estuarine valley is quite narrow (400–700 m) and relatively deep (10–20 m), with a relatively straight, north–south trend. This morphology developed as a consequence of fluvial incision during Quaternary time (Morales 1997; Boski et al. 2002). Plio-Quaternary synsedimentary tectonics

JOURNAL OF SEDIMENTARY RESEARCH, VOL. 73, NO. 6, NOVEMBER, 2003, P. 973–986
 1527-1404/03/073-973/$03.00

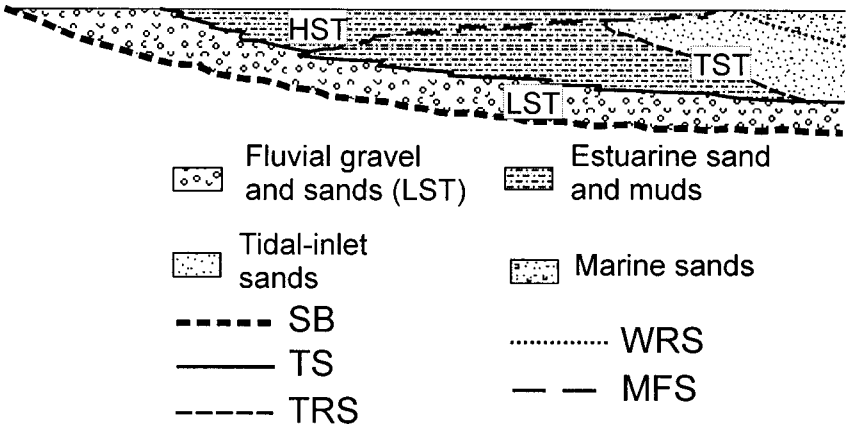

FIG. 1.—Stratigraphic model for sedimentary infill of present-day estuaries, with systems tracts and significant bounding surfaces. LST, lowstand systems tract; TST, transgressive systems tract; HST, highstand systems tract; SB, sequence boundary; TS, transgressive surface; TRS, tidal ravinement surface; WRS, wave ravinement surface; MFS, maximum flooding surface. Modified from Allen and Posamentier (1993) and Lessa et al. (1998).

are dominated by E–W and NNW–SSE trending fault systems in the area surrounding the Guadiana estuary, especially north of Ayamonte (Spanish Geological Survey 1983).

Hydrology

Fluvial Supply.—The Guadiana river is the main river of the southern part of the Iberian Peninsula, draining an area of 66,889 km^2 (Fig. 2). Mean annual water discharge is 144.4 m^3/s. This discharge is strongly dependent on rainfall, and, consequently, has a high daily, seasonal, and annual variability (Borrego et al. 1993). Together with the Guadalquivir River, the Guadiana River is the main sediment supplier to the adjacent Gulf of Cadiz margin. The estimated sediment supply over the last 44 years is 57.9×10^4 m^3/yr for suspended load and 43.96×10^4 m^3/yr for bed load (Morales 1993).

Tidal Regime.—The Guadiana mouth has a mesotidal regime, with a mean amplitude of around 2 m. Spring tides reach a maximum value of 3.4 m, with mean spring–neap tidal ranges of 2.82–1.22 m (Morales 1995). Mean velocities are 0.61 m/s during the flooding tide and 1.2 m/s during the ebbing tide (Instituto Hidrográfico 1998). Ebb currents occur for longer periods (6 h 50 min) than flood currents (5 h 35 min) (Morales 1993) (Fig. 3).

Wave Conditions.—The average significant wave height is approximately 0.8 m. Dominant waves approach from the southwest and west (about 50% of occurrences) (Borrego et al. 1993; Costa 1994), with heights not exceeding 0.5 m ($H_{1/3}$ = 0.4 m; T = 4.06 s) except during storm conditions. Southeasterly waves, with approximately 25% of occurrences, are more energetic ($H_{1/3}$ = 0.7 m; T = 5.08 s) (Costa 1994). The resulting net littoral drift is from west to east (Morales 1997).

Estuarine-Valley Stratigraphy

Several boreholes collected close to the estuarine valley show three main lithostratigraphic units (Boski et al. 2002): (1) a basal gravelly layer of fluvial origin overlying the Paleozoic basement (Unit I), with thickness of up to 35 m in the valley thalweg; (2) a 15–20 m thick mud-bearing unit with intercalation of fine and/or medium sand layers (Unit II); (3) a sandy unit up to 15 m thick (Unit III).

METHODOLOGY

About 250 km of high-resolution seismic profiles inside the Guadiana estuary were obtained parallel to and across the estuarine valley (Fig. 4) using a 3.5 kHz mud penetrator and a uniboom (Geopulse™: 280 Jul, shot delay of 500 ms, recording scale of 200 ms). An average velocity of 1500 m/s for time-to-depth conversions was used, providing minimum estimates of thicknesses of seismic units and depths to seismic horizons. Positioning was achieved by a differential GPS. Bathymetry was extracted from the

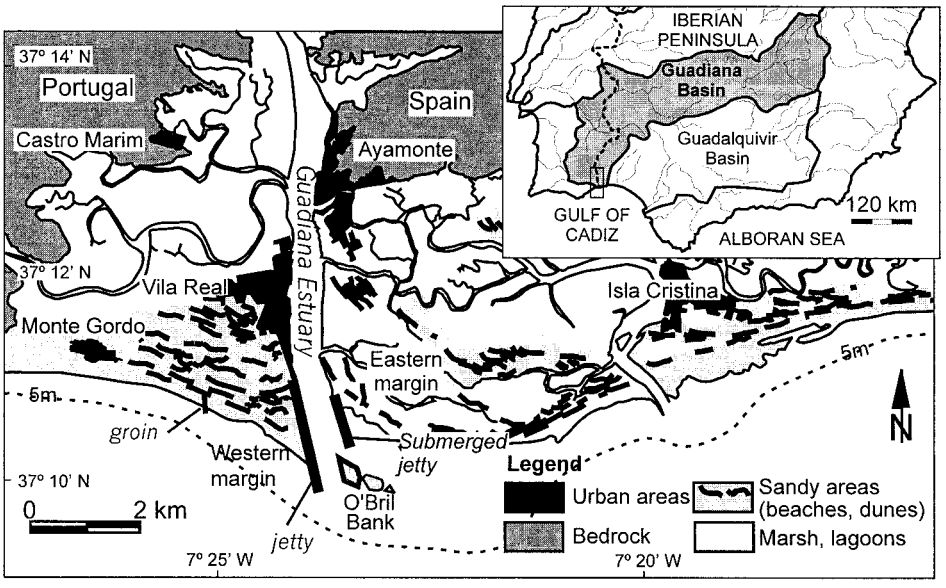

FIG. 2.—Guadiana estuary margins and location of the Guadiana drainage basin in the southern half of the Iberian Peninsula. Modified from González et al. (2001).

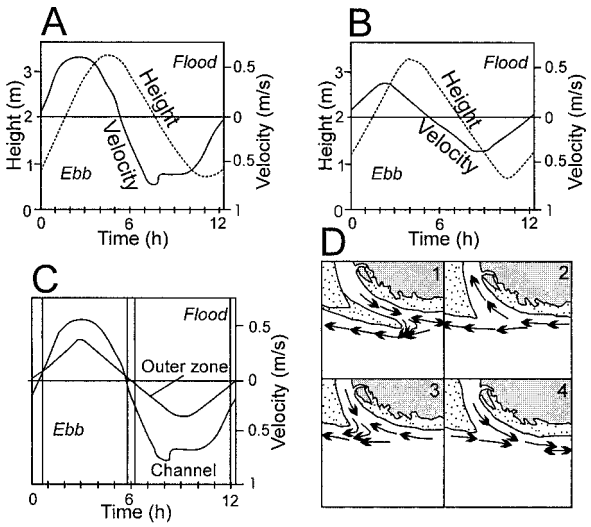

FIG. 3.—Present-day tidal regime of the Guadiana estuary mouth: **A)** tidal height and velocity currents during mean spring conditions in the estuarine valley; **B)** tidal height and velocity currents during mean spring conditions in the open coast in front of the estuary mouth; **C)** comparison between velocity–time curves; **D)** graphic model of current orientation during ebb and flood tidal conditions: 1) transition from ebb to flood conditions; 2) flood dominance; 3) transition from flood to ebb conditions; 4) ebb dominance. From Morales (1995).

physiographic map of the Guadiana river mouth, sheet 441A of the Spanish Hydrographic Institute.

The concepts of seismic stratigraphy were applied for the stratigraphic analysis, following their successful application to other shallow estuarine and valley-fill systems (Dalrymple and Zaitlin 1994; Thomas and Anderson 1994; Fenster and FitzGerald 1996; Lessa et al. 1998; Esker et al. 1998; Reynaud et al. 1999). The analysis was carried out by (1) identifying the key seismostratigraphic surfaces; (2) analyzing sediment-body geometries and seismic facies, and correlating them with stratigraphic units identified in boreholes; (3) interpreting depositional environments; and (4) recognizing the main structural elements, focusing on synsedimentary tectonics.

ESTUARINE SEDIMENTARY ARCHITECTURE AND EVIDENCE OF NEOTECTONIC ACTIVITY

The seismic stratigraphic analysis revealed five seismic units (SU 1 to SU 5 from oldest to youngest) recognizable throughout the study area. They locally overlie older units (Basal Units or BU) (Figs. 5, 6, 7). The lateral continuity of the estuarine units is interrupted by basement highs (BHs) generating positive estuarine bottom morphologies and characterized by a free-reflection acoustic response and a highly irregular relief. The main morphological characteristics of BHs are described in Table 1. Estuarine sectors located between the BHs were defined, beginning up-river, as A through D.

Basal Units (BU)

Seismic surveys usually penetrated the first 40–45 m, although seismic horizons were locally detected at depths of more than 60 m (Figs. 5, 6A), especially in the outermost sector (D). Three of these reflectors represent subhorizontal, high-amplitude erosional surfaces and display topographic irregularities 2–3 m high. These surfaces bound three seismic units (Basal Units A, B and C), up to 10 m thick, internally characterized by subparallel seismic reflectors, although their lateral continuity is frequently interrupted by uneven, contorted reflectors of moderately high amplitude (Fig. 6A). Their top boundaries are locally cut by channels (Fig. 6A). These deeper units are also recognized in the northernmost sector (A), where they display similar seismic configurations. Synsedimentary antiforms, possibly related to basement uplift, deform the basal units from the distal part of sector A to sector C. Inclined reflectors (0.6°) linked to the activity of more recent faults are common, especially near BH 4 (Fig. 6B).

Seismic Unit 1 (SU 1)

This seismic unit is bounded by seismic horizons SH 1 below and SH 2 above, except where SH 2 amalgamates with more recent horizons (Fig. 5). SH 1 is the first seismic surface showing lateral continuity. It is a moderate-amplitude to high-amplitude reflector amalgamating with younger horizons near the BHs (Fig. 6B, C). SH 1 deepens downstream throughout the study area, from 20–25 to 30 m (Fig. 5). Usually, this surface is highly irregular, with 0.5–1 km wide vertical morphological variations of 6–10 m (Fig. 8A). In the outer sector (D) this horizon is smoother, although there is a fault-enhanced low up to 8 m deep and 550 m wide southwards of BH 4 (Figs. 6B, 9). SH 1 is locally affected by more recent faults (Fig. 8A) with vertical offsets of up to 5 m (Figs. 5, 7A). However, locally some faults are also tapered by SH 1 (Figs. 6B, 7A).

Internally, SU 1 shows highly irregular, incoherent reflectors showing moderate to low lateral continuity and moderately high amplitudes (Fig. 6C). The acoustic response of this seismic unit is moderately reflective (Fig. 6C). SU 1 shows a uniform thickness of 4–8 m throughout the study area (Figs. 6A, 6C, 7B); however, it is locally thicker, up to 14 m in sector D, filling the depressions of SH 1 (Figs. 5, 8B). SU 1 thins to less than 4 m in several zones of distal sectors C and D, and it pinches out near BHs (Figs. 5, 6A, 8B).

Seismic Unit 2 (SU 2)

SU 2 is usually located between SU 1 and SU 3, but locally it can be overlain by SU 4 (Fig. 5). Seismic horizons SH 2 and SH 3 are its lower and upper boundaries, respectively. SH 2 is the most distinct high-amplitude reflector identified in seismic profiles (Fig. 6C). It is locally amalgamated with more recent horizons near topographic highs, irregularities, and BHs (Figs. 5, 6B). SH 2 is highly irregular, showing depth changes up to 8 m, and small-scale scours up to 5m high and up to 300 m wide (Fig. 7A), generally near BHs (Fig. 6C). Locally SH 2 can be subhorizontal, especially in sector D (Figs. 6A, 7A, 7B), where its depth increases downstream from 20 to more than 30 m (Fig. 8C). SH 2 is locally eroded by channels in the distal part of sector D (Fig. 5). Most neotectonic deformation identified in the study area is related to this stratigraphic level (Fig. 5). Faulting occurred particularly in parts of sector A, in sector C, with vertical displacements up to 4 m (Figs. 7A, 8C), and in sector D.

SU 2, particularly in sectors A and B, is seismically transparent and has internal subparallel and laterally continuous reflectors (Figs. 6A, 7B). In sectors C and D, low-angle (0.23–0.57°) northwards-directed progradational configurations are identified (Fig. 8D). SU 2 is normally 3–6 m thick, but it shows a variable thickness that is determined by underlying topography (Fig. 8D). The thickness reaches 12 m, where SU 2 fills SH 2 fault-enhanced topographic lows (Figs. 7A, 8D). SU 2 also shows small depocenters adjacent to BHs (Fig. 8D).

Seismic Unit 3 (SU 3)

SU 3 is generally bounded by horizons SH 3 and SH 4 (Fig. 5), except where they are missing. Its lower boundary (SH 3) is quite distinct in seismic profiles, because of low reflectivity of the underlying seismic unit (Fig. 6C) and its erosional character in many sections (Fig. 7A). In some places it amalgamates with SH 2, mainly near BHs, and with SH 4. SH 3 is generally located at depths of less than 20 m (Figs. 6A, 8E). Erosive scours 3–4 m high and 100–200 m wide are quite common, especially close to BH 3 and BH 4 (Fig. 8E). Locally, SH 3 also marks the base of erosional

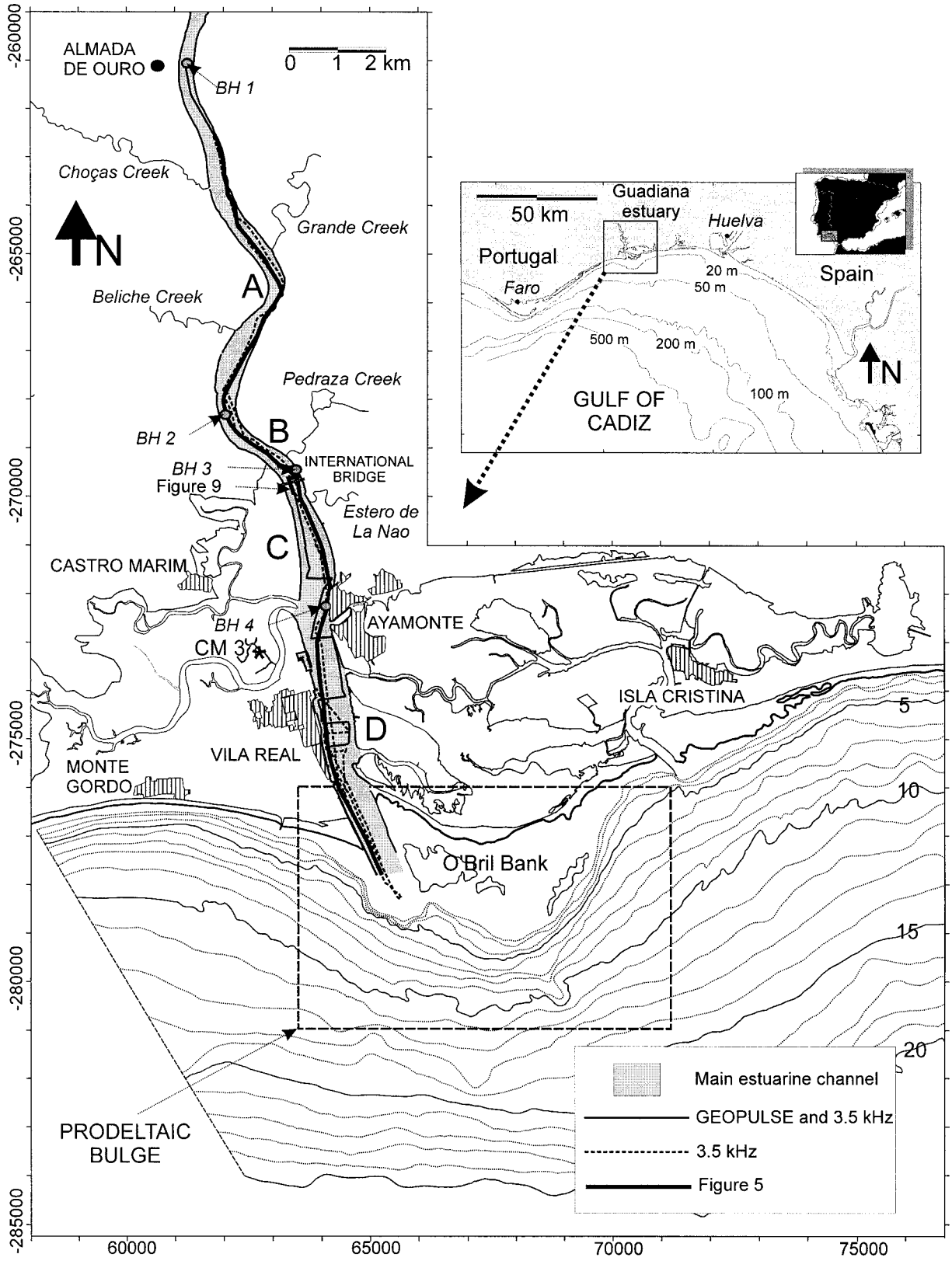

FIG. 4.—General location of high-resolution seismic profiles in the lower part of the Guadiana valley with indication of basement highs (BHs) and adopted zonation (A to D). The location of borehole CM 3 is also depicted. Bathymetric contours (in meters) are represented for the adjacent infralittoral and inner shelf in front of the Guadiana estuary, evidencing a bathymetric protuberance associated with a submarine prodelta.

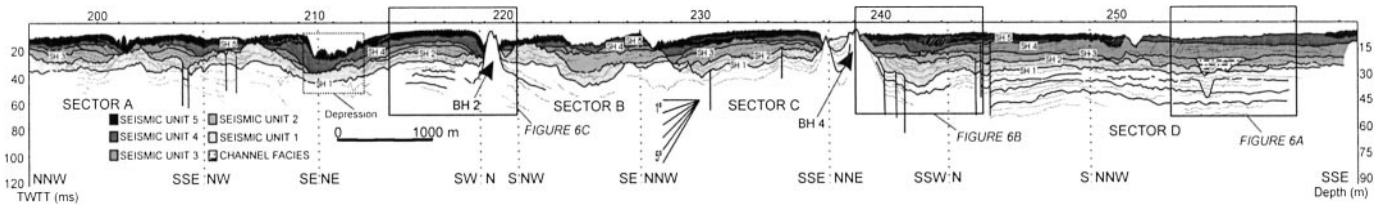

FIG. 5.—General seismic profile across the lower part of the Guadiana estuary. Several basement highs (BHs) are identified. Seismic units (SU) and horizons (SH) are identified along the entire seismic section. Vertical dotted lines indicate changes of orientation. Position of this seismic section is indicated in Figure 4.

scours and channels 3–10 m deep and 100–800 m wide (Figs. 5, 6C, 8E). Recent faulting deformed SH 3 in sector D (Figs. 5, 6B).

SU 3 shows a highly reflective acoustic response and generally lacks internal reflectors (Fig. 6B, C). However, internal configurations are locally observed (Fig. 6A), as in sector A, where low-angle progradational reflectors (2.29°) are identified, and in sector D, where up-estuary-directed reflectors decrease their angle progressively from 3.43° to 0.57° (Fig. 8F). SU 3 gets thinner (2–5 m thick) and discontinuous upstream, as it is usually identified south of older topographic highs (Figs. 5, 6C, 8F). SU 3 displays the most significant thickness in sector D. Here, it forms a lenticular body up to 8 m thick that thins landward and towards the river mouth (Figs. 6A, 8F). This depocenter was cut by more recent channels; some of these have recently been filled (Fig. 8F).

Seismic Unit 4 (SU 4)

The lower and upper boundaries are seismic horizons SH 4 and SH 5 (Fig. 5). SH 4 amalgamates with older surfaces, especially with SH 2, and with the estuary bottom (Fig. 7A). SH 4 is generally subhorizontal, with erosional scours 1–2 m deep and channels up to 5 m deep and 600 m wide, particularly adjacent to BH 4 (Figs. 5, 6B, 8G). SH 4 is located progressively deeper towards the river mouth (Fig. 8G). An undulating pattern related to this horizon is observed in sector D (Fig. 5).

The thickness of SU 4 is moderate (3–4 m), although it can reach up to 15 m and averages 7–8 m in depressions and channels (Figs. 6B, 7A, 8H). SU 4 is also significantly thicker (up to 9 m) close to BHs (Fig. 6C), and in sector D, where a wedge up to 6 m thick can be recognized (Figs. 6A, 8H). SU4 is absent on top of topographic elevations. This unit is locally eroded by SH 5 or the present-day topography. SU 4 has a moderately reflective acoustic response (Fig. 6B). Seaward-directed internal progradational patterns with angles usually higher than 3.5° are locally observed. A radial pattern can be detected in sector D, with lateral accretion and landward-directed progradation (0.76°) (Figs. 7B, 8H). Low-angle (0.20°) seaward-progradational patterns with high lateral continuity are identified in the distal part (Figs. 6A, 8H).

Seismic Unit 5 (SU 5)

This is the most recent unit in the study area. It is generally located at topographic elevations overlying SU 4 (Fig. 5) but locally overlies older units. Its lower boundary is horizon SH 5 (Fig. 5), which amalgamates with older surfaces (Fig. 7A). Generally, SH 5 is a regular, subhorizontal reflector (Fig. 8I), with only local irregularities, particularly close to BHs (Figs. 6B, 8I). Seaward, SH 5 shallows to 10–11 m (Figs. 7A, 8I). The upper boundary of SU 5 is the present-day estuarine bottom, which is

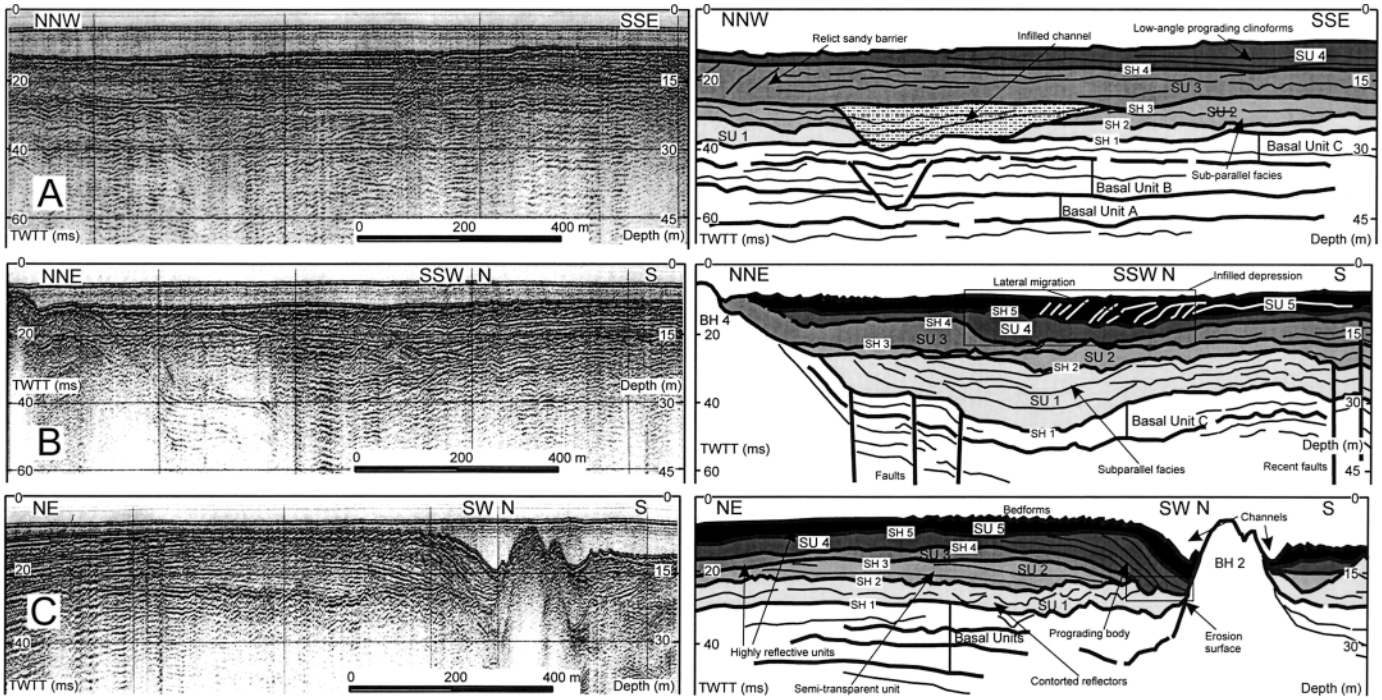

FIG. 6.—Seismic and interpretative sections in the Guadiana estuary. Positions are indicated in Figure 5. **A)** Outermost zone of sector D. **B)** Sector D, close to BH 4. **C)** Sector A, close to BH 2.

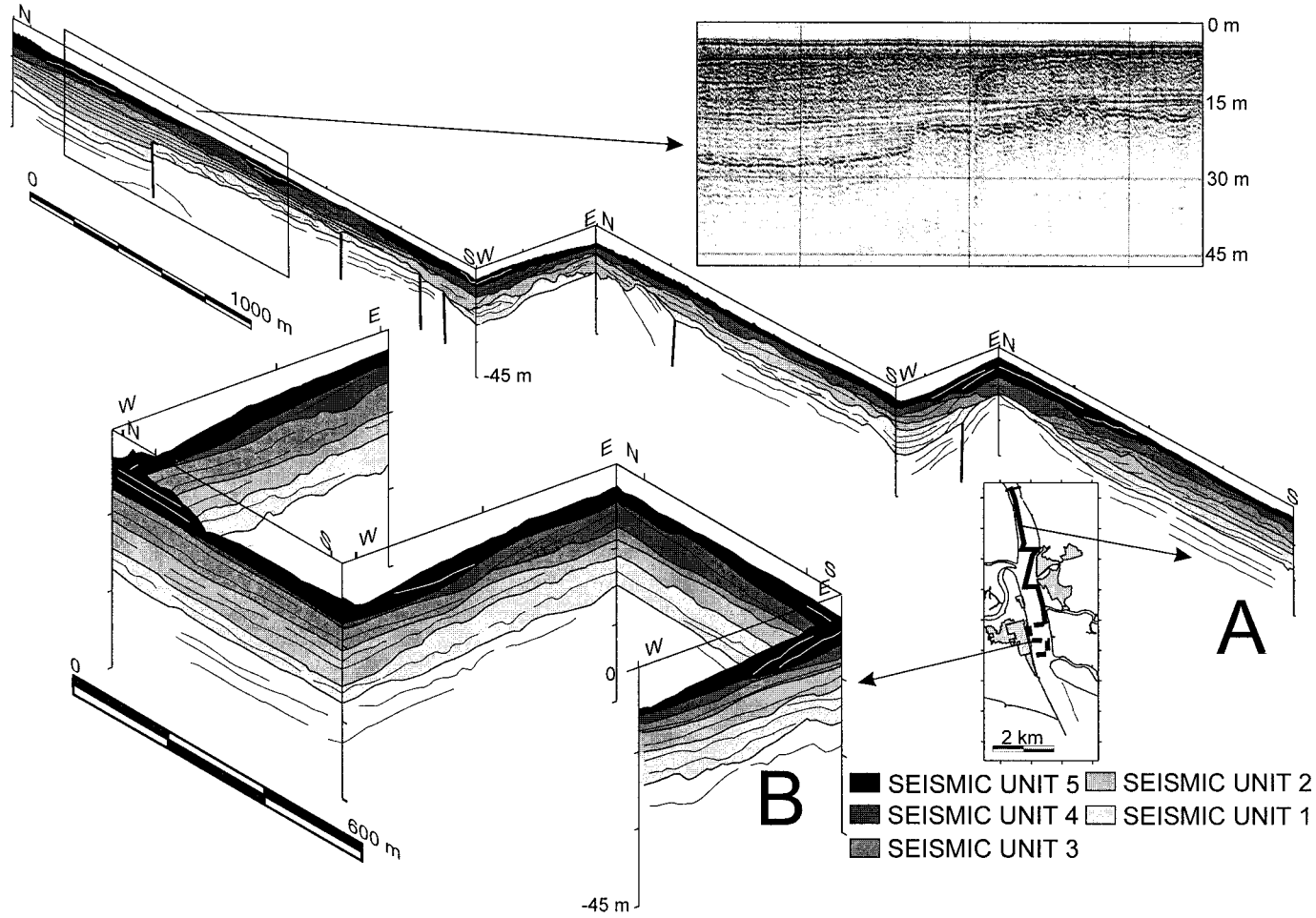

FIG. 7.—Fence diagrams of estuarine sedimentary infill, showing lateral relationships between seismic units and horizons. **A)** Interpretive sections in sectors C and D; note neotectonic activity affecting SU 5. **B)** Interpretive sections close to river mouth.

molded by bedforms 2–3 m high (Fig. 6C). Other surface features such as scours and/or bedforms are evident north of BH 2 (Fig. 5).

SU 5 has a highly reflective acoustic response (Fig. 6C), with landward and lateral progradational patterns in distal sectors (C and D). Channel migration can be identified locally (Figs. 6B, 8J). SU 5 is interrupted laterally by BHs and by channels (Figs. 6C, 8J). It is up to 6 m thick, with maximum thickness in morphological depressions (Figs. 7A, 8J).

SEQUENCE STRATIGRAPHY OF THE GUADIANA ESTUARY

The basis for establishing a sequence stratigraphic framework and inferring depositional environments was the correlation between the seismic stratigraphic units defined in the estuarine valley and the stratigraphic section of the Guadiana estuary defined through borehole data (Boski et al. 2002) (Fig. 9). Particularly, borehole chronostratigraphic data based on the ^{14}C method of the late Quaternary succession prior to the Holocene highstand (Boski et al. 2002) were used as reference for interpretations presented here. In addition, the analysis of progradational trends, seismic stacking pattern, and particularly the character of seismic horizons in valley fills allowed a correlation between estuarine stratigraphy and: (1) late Quaternary sea-level highstands evidenced in glacio-eustatic sea-level curves (Shackleton 1987; Bard et al. 1990; Berger 1992); (2) late Quaternary sea-level falls and lowstands registered on the offshore shelf (Somoza et al. 1997; Hernández-Molina et al. 2000; Lobo et al. 2002); and (3) Holocene highstand sea-level changes documented in nearby estuarine and coastal Gulf of Cádiz systems (Borrego et al. 1993; Zazo et al. 1994; Zazo et al. 1996; Goy et al. 1996; Rodríguez-Ramírez et al. 1996; Dabrio et al. 2000). Integration of all information produced the sequence stratigraphic interpretation of the sedimentary fill of the Guadiana estuary presented in Figure 10.

TABLE 1.—*Main morphological parameters of basement highs (BHs) identified in the study area.*

BH	Height	Minimum Depth	Lateral Extension	Lateral Channels
1	3 m	7 m	100 m	No
2	9 m	5 m	150 m	Yes
3 (Double outcrop)	4 m and 6 m	12 m and 8 m	100 m and 50 m	No
4 (Double outcrop)	5 m in both cases	5 and 9 m	50 m in both cases	Yes

Basement Morphology and Faulting

Free-reflection acoustic responses identified at the base of the estuarine fill of the Guadiana estuary are indicative of basement rocks (cf. Fenster and Fitzgerald 1996) and are thought to represent Paleozoic basement, Mesozoic, and Tertiary rocks. They constitute topographic highs, such as BHs 3 and 4, generally located at the margins of the estuarine valley, indicating that the location of the valley is strongly constrained by basement elevations. Significant scouring occurred around these highs, suggesting that estuarine flows were diverted by the highs and erosion preferentially removed sediment close to the elevations.

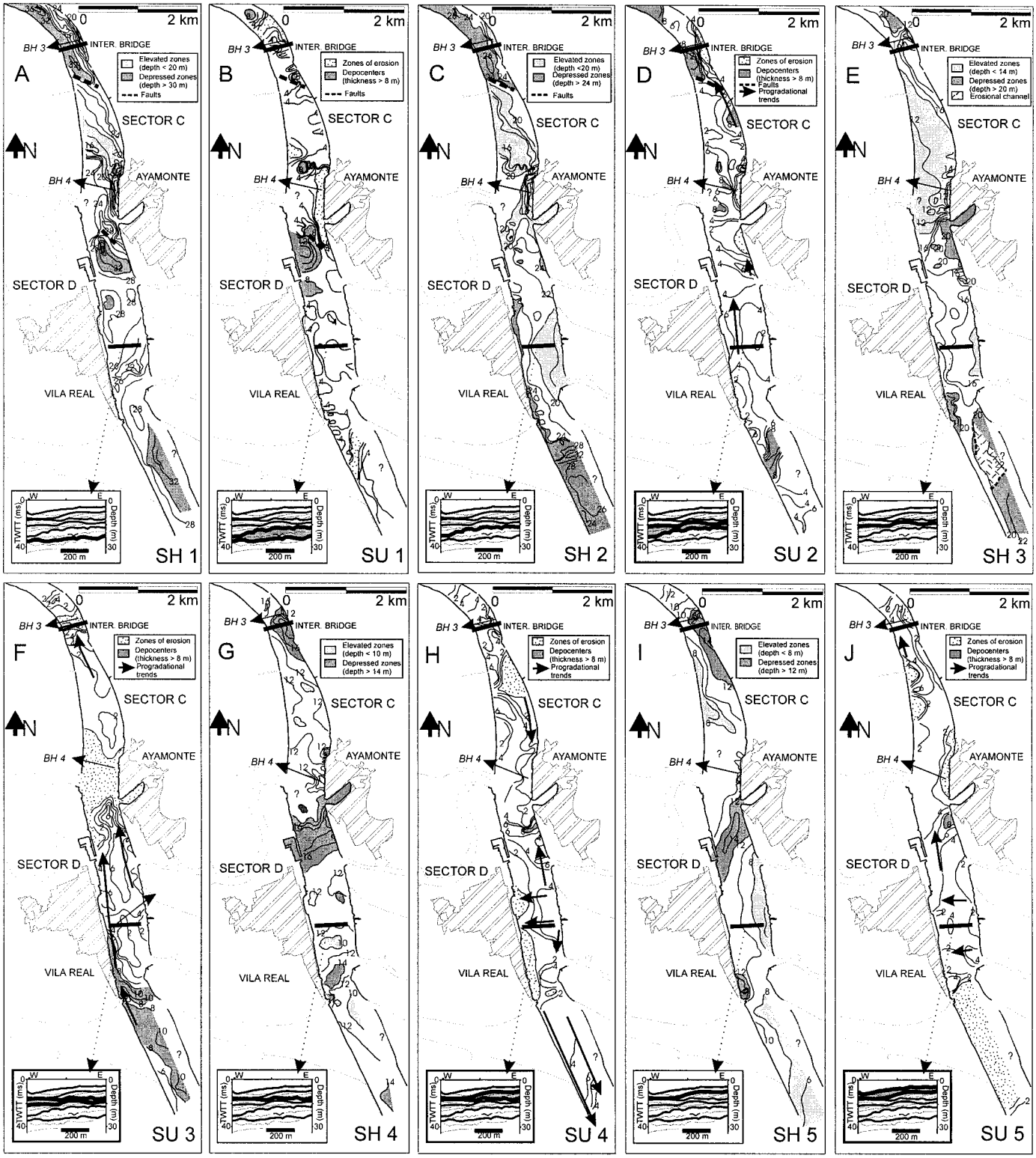

FIG. 8.—Distribution of seismic horizons (SHs) and units (SUs) southward of the International Bridge (A to J). All values are given in meters: depth for seismic horizons and thickness for seismic units.

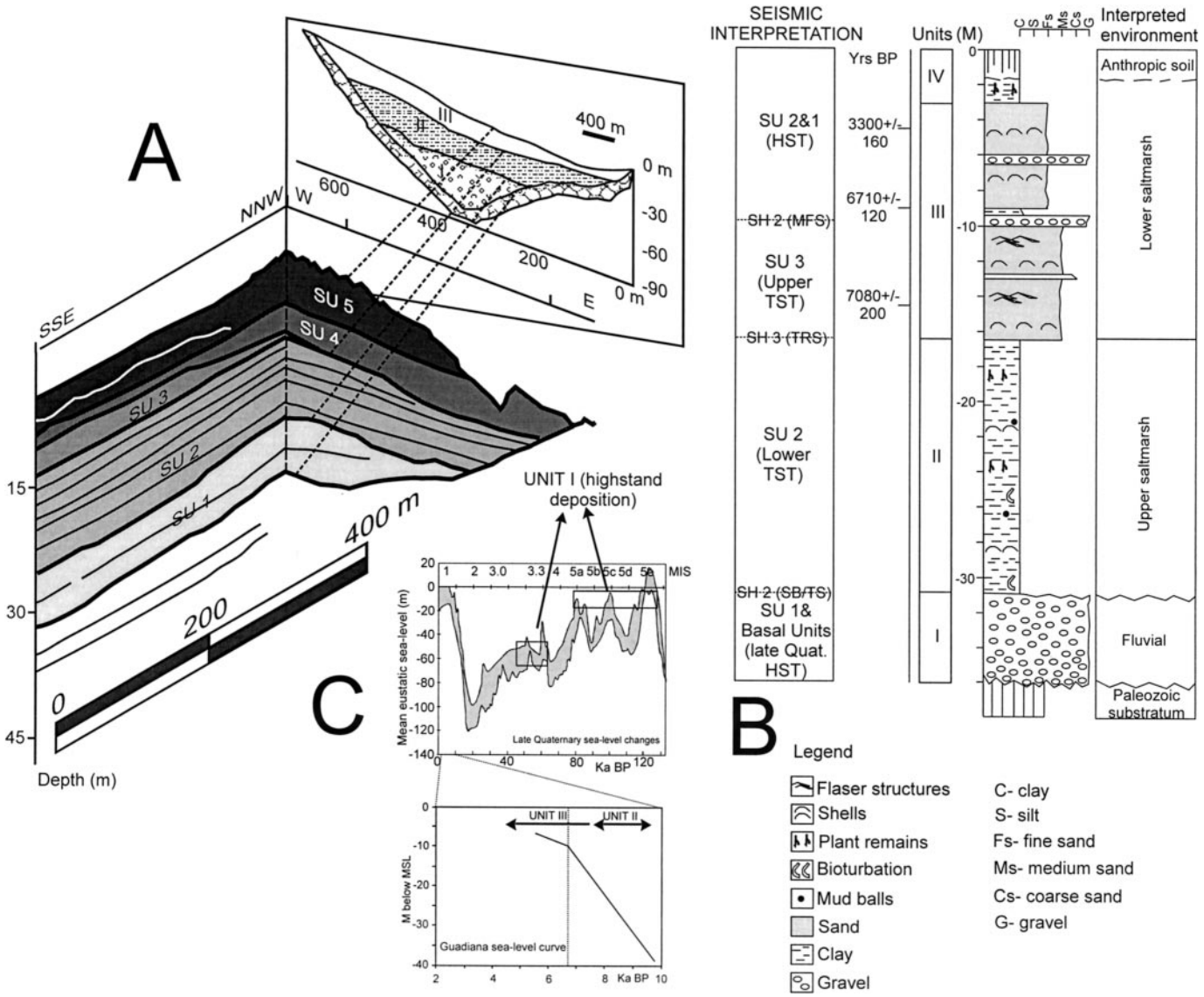

FIG. 9.—Correlation between the seismic stratigraphy (A) of the Guadiana estuary and the valley margin stratigraphy (B) at borehole CM 3 (See position in Figure 4), with indication of lithologic units (I, II, and III) chronostratigraphy (C) from stratigraphic data of Boski et al. (2002). Late Quaternary sea-level changes were depicted considering a band between maximum and minimum estimate, from different late Quaternary sea-level curves (Shackleton 1987; Bard et al. 1990; Berger 1992). Guadiana sea-level curve is from Boski et al. (2002).

Some faults identified in the seismic records seem to display a NNW–SSE to NW–SE trend (Fig. 8A, B), similar to the fault trend recognized on outcrops along the estuarine valley. These structures probably originated during the Hercynian orogeny but were reactivated during late Pliocene and Quaternary times (Spanish Geological Survey 1983). The data presented here provide clues about the timing of Quaternary movements (Table 2) and are in good agreement with previous work that suggest that faults in southwestern Spain ceased moving before the Holocene (Zazo et al. 1999).

The Sedimentary Architecture of the Guadiana Estuary

Basal Units and SU 1: Late Quaternary Highstand Deposits.—The basal fluvial deposits of estuarine successions are usually considered to be generated during lowstands or during the initial phases of transgression (Dalrymple et al. 1992; Allen and Posamentier 1993). In the Guadiana estuary, instead, ^{14}C dating links the basal fluvial deposits of Unit I with Isotope Stages 5 and 3 highstands (Boski et al. 2002), analogous to the fluvial record present in the nearby Guadalete estuary (Spanish coast of the Gulf of Cadiz) and ascribed to Isotope Stage 3 (Dabrio et al. 2000). Isotope Stage 3 highstand deposits were also observed on the Gulf of Cadiz shelf (Hernández-Molina et al. 2000; Lobo et al. 2002).

The results obtained from the seismic stratigraphic analysis agree with these data. SH 2, the most distinct, recognizable stratigraphic surface identified in the sedimentary fill of the Guadiana estuary, can be used as a stratigraphic marker. This reflector represents a clear facies transition from predominantly incoherent facies patterns of SU 1 to semitransparent facies of SU 2. The strong seismic signature, the common occurrence of depressed morphologies, and the highly irregular and erosional pattern of SH 2 are diagnostic criteria indicating subaerial exposure and erosion during the sea-level fall and lowstand of $\delta^{18}O$ stage 2, in agreement with the interpretations made by numerous authors (e.g., Thomas and Anderson 1994; Nichol et al. 1996; García-Gil et al. 1999; Lerocolais et al. 2001) (Table 2).

Units underlying SH 2 (Basal Units and SU 1) show similar stratigraphic

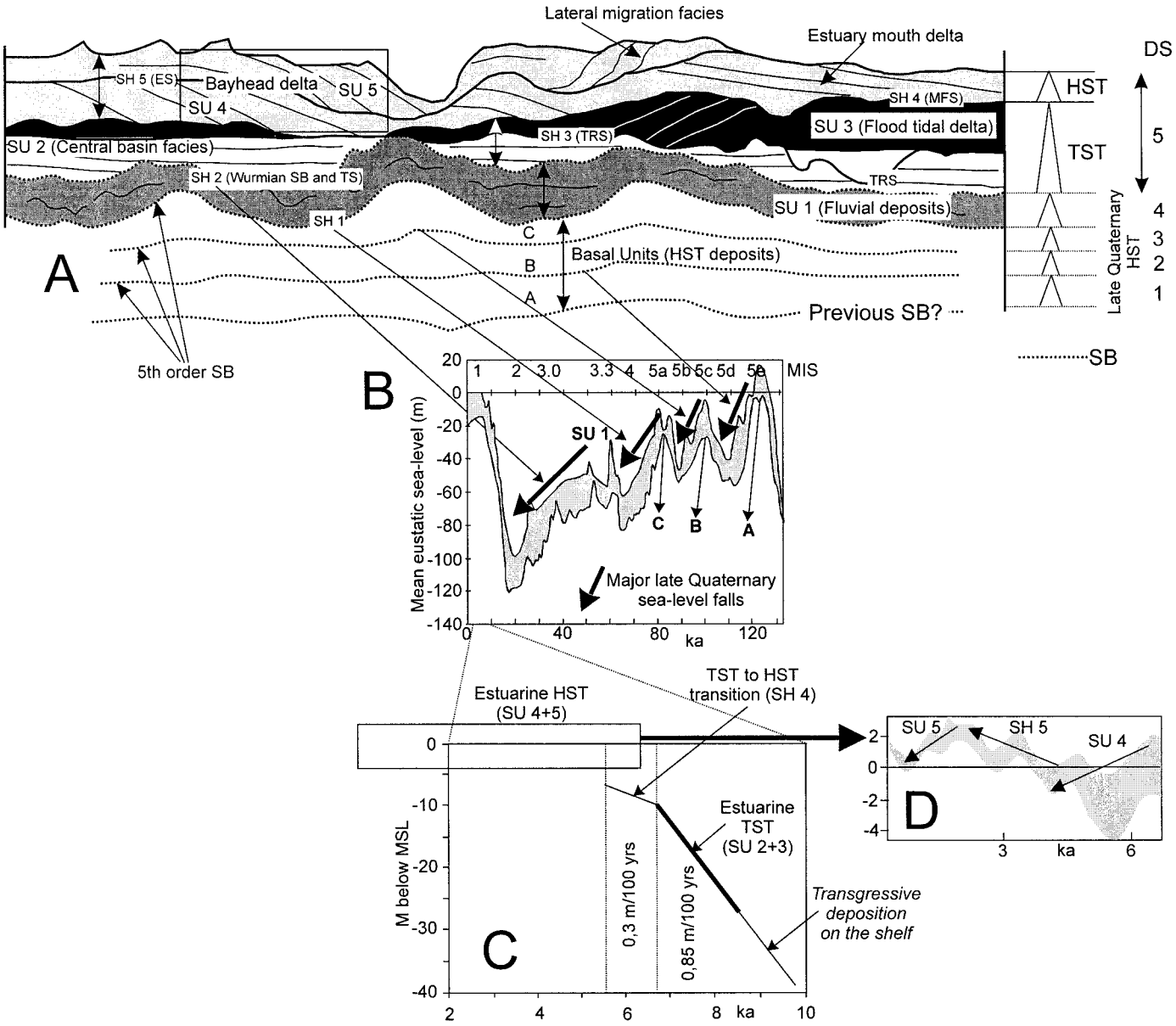

FIG. 10.—**A)** Proposed sequence stratigraphic model of the Guadiana estuary sedimentary fill and **B)** correlation with late Quaternary sea-level changes (Shackleton 1987; Bard et al. 1990; Berger 1992), **C)** Guadiana sea-level curve (Taken from Boski et al. 2002), and **D)** Holocene highstand sea-level changes (Taken from Somoza et al. 1998). This interpretation is based on the chronostratigraphic framework provided by the correlation between estuarine seismic units and the estuarine stratigraphic section, and also by the link established between high-amplitude reflectors and significant sea-level falls. Legend: TST, transgressive systems tract; HST, highstand systems tract; SB, sequence boundary; TS, transgressive surface; TRS, tidal ravinement surface; MFS, maximum flooding surface; ES, erosion surface: MIS, marine isotopic stages; DS, depositional sequence; MSL, mean sea level.

features, such as the common occurrence of discontinuous, contorted, and moderately high-amplitude reflectors. These types of seismic configurations are characteristic of lower units of valley infills and are considered to represent fluvial deposits at the bases of estuarine successions (Brown and Fisher 1985; Esker et al. 1998; Lericolais et al. 2001). Correlation with core data indicates that these facies are composed of fluvial gravels and coarse sands (Unit I in the stratigraphic section) and can be linked to Substages 5e, 5c, and 5a and Isotope Stage 3 highstands (Fig. 10, Table 2) (Shackleton 1987; Bard et al. 1990; Berger 1992). The highly irregular SH 1 and the surfaces that separate the Basal Units can be therefore linked to the fifth-order glacio-eustatic sea-level falls (Substages 5d, 5b, and Isotope Stage 4) that occurred between these highstands (Fig. 10). Because of the asymmetric character of these fifth-order sea-level cycles, the falling segments of the glacio-eustatic curve were more prolonged than subsequent sea-level rises (Chiocci et al. 1997). Consequently, subaerial exposure and erosion of previously formed highstand deposits was favored. Data from the late Quaternary record of the adjacent shelf support this interpretation. This shelf shows dominance of prograding sedimentary wedges interpreted as regressive to lowstand deposits formed during fifth-order sea-level cycles between Isotope Stages 5 and 3. These wedges are bounded by fifth-order sequence boundaries that can be traced landward and which show local occurrence of incised channels (Somoza et al. 1997; Hernández-Molina et al. 2000).

The stronger seismic signature of SH 2 is related to a more significant sea-level fall ($\delta^{18}O$ stage 2) (see Fig. 10). Multiple sequence boundaries in incised-valley systems are not uncommon and have been documented in

TABLE 2.—*Summary of main evolutionary steps recorded in the sedimentary infill of the Guadiana estuarine valley showing the relationships with estuary-margin stratigraphy, shelf processes, and neotectonic movements. An estimated timing of events is reported.*

Evolutionary Steps: Dominant Estuarine Processes	Estuarine Seismic Stratigraphy	Estuarine Stratigraphic Section (Boski et al. 2002)	Shelf Evolution (Somoza et al. 1997, Hernández-Molina et al. 2000, Lobo et al. 2001, 2002)	Tectonic Activity	Sea-Level Trend/ Estimating Timing
1) Late Quaternary sedimentation; Deposition of fluvial deposits during highstands, formation of fifth order sequence boundaries during sea-level falls and lowstands	Basal Units and SU 1	Marsh deposits	Shelf starvation, deposition only during Isotope Stage 3	Evidence of folding and faulting	Highstand periods (Isotope Stages 5 and 3)
2) Formation of the last fifth order sequence boundary: Non-deposition site; channel bypass, seaward sediment transport	SH 2	Not identified	Two periods: i) formation of regressive and lowstand deposits; ii) Deposition of transgressive bodies	Pre-Holocene faulting activity generated small- and medium-scale depressions in the estuarine channel	Two intervals: i) Sea-level fall and Würmiam lowstand (Isotope Stage 2): −120 m minimum sea-level (Dias et al. 2000); ii) Sea-level rise during the post-glacial transgression (after 18 ka)
3) Estuarine flooding: Development of relatively deep-water conditions, accelerated estuarine infilling; deposition of mud-dominated central basin facies	SU 2	Development of extensive tidal flats and marshes	Shelf starvation, sedimentation processes greatly reduced	Fault-controlled depressions acted as preferential sites of deposition; minor neotectonic activity	Upper part of postglacial transgression [after 9.8 ka according to Boski et al. (2002), and after 8.5 ka according to Lobo et al. (2001)]. Sea-level rise rate of 0.85 m/century (Boski et al. 2002).
4) Generation of a tidal ravinement surface (TRS) i) Outer zones: development of significant tidal channels; ii) Inner zones: strong erosional processes near basement elevations, possibly due to the intensification of current flows and to the increased velocity caused by bathymetric constraints.	SH 3				
5) Deposition of sandy transgressive deposits, decrease of accommodation space enhanced reworking processes: i) Outer zones: deposition of estuary-mouth sands; ii) Inner zones: introduction of sandy deposits, associated with the enhanced activity of flood tidal currents caused by tidal prism increase	SU 3	Coarse sedimentation		No evidences of neotectonic activity	Final stage of postglacial transgression (7.5–6.5 ka), in relation to maximum retrogradation of estuarine barriers (Dabrio et al. 2000; Boski et al. 2002)
6) Maximum estuarine flooding: Generation of a maximum flooding surface (MFS) in relation to the complete drowning of the estuary, renewed activity of tidal currents	SH 4	Not identified			Transition between transgressive and highstand conditions (6.5–5 ka). Sea-level rise rate of 0.3 m/century (Boski et al. 2002)
7) Early Highstand: Downstream sediment transport, increased seaward progradation and ebb tidal activity; formation of bay-head delta (point bars, tidal bars, lateral accretion bars), initiation of estuary-mouth delta	SU 4	Formation of: i) Estuarine and point bars; ii) Littoral spits at the estuary mouth	Submarine deposits located close to the river mouth began to acquire a deltaic morphology (Morales 1993). Two main progradational intervals defined on the shelf domain		Sea-level stabilization and/or subtle fall between 5 and 2.5 ka (Goy et al. 1996; Dabrio et al. 2000)
8) Generation of a nondepositional surface, delta lobe switching possibly involved?	SH 5				Small sea-level rise at around 2.5 ka (Goy et al. 1996; Dabrio et al. 2000)
9) Late Highstand: Local erosion and/or migration of tidal channels, lateral accretion and development of tidal bars and channel facies, continuation of estuary-mouth delta construction	SU 5				Sea-level stabilization and/or subtle fall, from 2.5 ka to the present (Goy et al. 1996; Dabrio et al. 2000)

older deposits, such as the Trinity–Sabine complex (Thomas and Anderson 1994) or the Lake Calcasieu estuary (Nichol et al. 1996).

SU 2 and SU 3: Holocene Transgressive Deposits.—The basal part of the transgressive systems tract (TST) is represented by Seismic Unit 2 (SU 2), whose lower boundary represents the Würmian sequence boundary but also the transgressive surface, generated during estuary flooding (Fig. 10, Table 2). SU 2 is characterized by a low reflectivity and a distinct seismic configuration, showing continuous, parallel and planar reflectors. These diagnostic seismic features have been correlated in other valley fills where cores are available. The parallel reflectors consist of muds with fine sand intercalations, interpreted as estuarine muds or central-bay facies (Thomas and Anderson 1994; Fenster and Fitzgerald 1996; Esker et al. 1998; Reynaud et al. 1999). According to this, SU 2 is correlated with Stratigraphic Unit II, which is a thick clay interval deposited during the last phases of postglacial transgression between 9.8 and 7.5 ka (Boski et al. 2002). Presence of main faults affecting the lower boundary of SU 2 also supports the development of SU 2 during the early Holocene, inasmuch as the main fault movements in this area are considered to be pre-Holocene (Zazo et al. 1999). Consequently, SU 2 is interpreted as a muddy, postglacial transgressive deposit of estuarine nature (Figs. 9, 10). The upper boundary of SU 2 is erosional (SH 3), and it shows the presence of channel forms cut onto the lower transgressive muddy deposit. SH 3 is considered a tidal ravinement surface, generated by tidal action during progressive coastline migration (cf. Dalrymple et al. 1992; Reynaud et al. 1999). Consequently, an offshore origin is not favored for those muddy deposits, because major tidal ravinement is expected to occur in semi-enclosed basins, typically in estuarine environments where tidal amplification has been documented (Larcombe and Jago 1994).

The upper component of the estuarine TST is usually generated by landward-prograding coastal barriers and/or flood tidal deltas (Thomas and Anderson 1994; Saito 1995), generating a coarsening-upward sequence inasmuch as they usually overlie finer estuarine deposits. This pattern is evidenced within SU 3, interpreted as the upper component of the TST (Fig. 10). The specific seismic and morphologic features of SU 3, such as high reflectivity and faint stratification, occurrence of landward-dipping clinoforms downlapping onto central bay facies, identification of toplap terminations, and lenticular external shape in the outer sector, have been attributed in other valley fills to landward progradation of flood tidal deltas or washover fans (Dalrymple and Zaitlin 1994; Thomas and Anderson 1994). This interpretation is supported in the study area by correlation between SU 3 and the sandy deposits of Unit III measured in the estuary margin (Fig. 9). The lithologic change observed between Unit II and Unit III (Fig. 9) may account for the reflectivity increase observed from SU 2 to SU 3. Stratigraphic information from nearby coastal embayments of the Gulf of Cadiz, such as the Cadiz Bay, shows an equivalent landward-prograding body (Dabrio et al. 2000).

SU 4 and SU 5: Holocene Highstand Deposits.—The composition of the estuarine highstand is variable but usually comprises bay-head delta deposits, generated as decreasing rates of sea-level rise allowed sediments to be deposited inside the estuary (Dalrymple et al. 1992; Saito 1995). In the Guadiana estuary, these deposits consist of SU 4 and 5, because (Fig. 10): (1) The common identification of seaward-directed prograding inner estuarine facies related to SU 4 constitute a change from the underlying unit (SU 3), because they are indicative of the construction of a bay-head delta (cf. Dalrymple and Zaitlin 1994; Nichol et al. 1996), probably consisting of tidal bar deposits. The formation of such deposits has been linked in other studied estuaries with initial rapid fill and downstream sediment transport following the maximum Holocene flooding (Fenster and FitzGerald 1996). (2) Their highly reflective pattern indicates that they are dominated by sand (cf. Fenster and FitzGerald 1996). (3) Lateral progradation is linked to the formation of lateral accretion deposits, characteristic of highstand stabilization (cf. Woodroffe et al. 1989). In addition, the Guadiana estuarine-margin stratigraphy shows the dominance of sandy sedimentation (unit III) characterized by progradational phases with point bars and tidal bars during this final interval (Boski et al. 2002) (Fig. 9).

The existence of cyclic sedimentation in the Guadiana estuary during the last highstand interval, which began at about 6.5–6 ka after the maximum flooding, can be related to phases of major progradation recognized in several estuaries and embayments of the Gulf of Cadiz (Borrego et al. 1993; Zazo et al. 1994; Zazo et al. 1996; Goy et al. 1996; Rodríguez-Ramírez et al. 1996; Dabrio et al. 2000). The progradational phases have been related to stillstands followed by subtle sea-level falls, in turn related to climatic transitions (Goy et al. 1996; Rodríguez-Ramírez et al. 1996; Zazo et al. 1996). These phases are believed to indicate two main sea-level oscillations since the Holocene maximum (Zazo et al. 1996) and have been recognized in other shallow marine deposits around the Iberian Peninsula (Hernández-Molina et al. 1994; Hernández-Molina et al. 2000; Somoza et al. 1998; Lobo 2000).

The first progradational interval (Early Highstand, represented in other Gulf of Cadiz coastal settings by H_2 Unit) is believed to have occurred after 5 ka (Goy et al. 1996; Dabrio et al. 2000). Formation of SU 4 may be related to this first progradational interval (Table 2), which was preceded by a transition between transgressive and highstand conditions (6.5–5 ka). This transition was characterized by a reduced rate of sea-level rise and by attenuated sedimentation or erosion (Boski et al. 2002). The transition is marked by SH 4, which is a downlap surface (DLS) interpreted as the MFS (Fig. 10), reflecting the progradation of funnel sediments over estuary-mouth sands.

The first progradational period was interrupted at ca. 2.5 ka (between 2.7–2.3 ka according to different authors), by a sea-level rise documented in several Gulf of Cadiz littoral formations (Goy et al. 1996; Rodríguez Ramírez et al. 1996; Zazo et al. 1996). In addition, numerous evidences of the occurrence of a transgressive period during the middle part of the Holocene highstand are reported from relatively nearby environments, such as shelf deltaic deposits around Spain (Hernández-Molina et al. 1994; Hernández-Molina et al. 2000; Somoza et al. 1998), estuarine sequences in northern Spain (Cearreta 1994; Pascual et al. 1998), and the Gironde estuary in southwestern France (Massé et al. 2000; Clavé and Massé in press). Because SH 5 does not show widespread erosion and is mostly regular, it is considered a nondepositional surface. Therefore, it seems logical to relate the formation of this surface with the reported Holocene mid-highstand transgression, which led to interruption of sedimentation in the Guadiana estuary (Table 2). In addition, the common identification of toplap terminations and the low extension of erosion associated with this surface does not support an origin related to a sea-level fall.

The second progradational interval (Late Highstand, represented by units H_3 and H_4 in nearby Gulf of Cadiz settings) is supposed to have occurred after 2.5 ka and was characterized by renewed progradation of littoral spits and by progradation of the tidal flat in relation to delta construction (Goy et al. 1996; Dabrio et al. 2000). It is represented by SU 5 (Table 2).

DISCUSSION

This study provides new clues as to the seismic characterization of estuarine systems tracts and their boundaries in narrow, bedrock-controlled estuaries, characterized by moderate episodic sediment supply, and also with regard to the preservation potential of estuarine sequences and their relation to sea-level changes. Distinctive sequence stratigraphic features of the Guadiana incised-valley fill are described below.

Nature of Estuarine Fill: Preservation Potential of Estuarine Sequences

The lower part of the Guadiana estuarine fill (Basal Units and SU 1) is interpreted to consist of four fifth-order sequences, which are composed of highstand deposits (Fig. 10). During periods of late Quaternary sea-level fall and lowstand (Fig. 10), bypassing was probably dominant in the valley, inasmuch as the lowering of the base level and the narrow morphology favored subaerial exposure and the generation of erosion surfaces rather than estuarine sedimentation. The identification of thick regressive lowstand wedges in the adjacent middle to outer shelf supports this interpretation (Somoza et al. 1997; Hernández-Molina et al. 2000). Periods of sea-level rise prior to the Last Glacial Maximum were too rapid to allow significant deposition in the valley, and preservation of transgressive deposits seems related to the last phase of postglacial transgression, when sea-level rise was large enough to flood the estuarine valley (Lobo et al. 2001). Late Quaternary periods of highstand sea-level stabilization permitted significant sedimentation (Dabrio et al. 2000; Boski et al. 2002). Because of their location in a protected, bedrock-controlled setting, these highstand deposits would have been only partially removed during subsequent sea-level falls. In contrast, coastal deposits underwent significant erosion laterally (Lobo 2000). Finally, the last fifth order depositional sequence also records part of the Holocene highstand in the estuarine valley. Therefore, it seems that estuarine highstand deposits have the greatest preservation potential.

Estuarine Sedimentation during the Last Glacial Maximum

The Guadiana estuarine valley is characterized by poorly developed fluvial deposits during the Last Glacial Maximum (Würm) and the initial postglacial transgressive stages. This can be attribute to: (1) Low sediment supply from the Guadiana river and tributaries. Estuaries characterized by thick basal lowstand fluvial deposits related to the last lowstand and/or postglacial transgression received much higher sediment supply (Saito 1995; Zhang and Li 1996; Hori et al. 2001) than estuaries with poorly developed fluvial deposits (Lessa et al. 1998); (2) Narrow valley morphology. Incision of the Guadiana estuary into rocky substrate created a narrow morphology that did not favor accumulation of muds in tidal flats and marshes but promoted bypass of the estuarine central basin (cf. Nichol et al. 1996) and deposition in the marine environment (Borrego et al. 1995); (3) Low tectonic subsidence of the Guadiana area, which behaved as a morphostructural high during late Quaternary (Lobo 2000; Lobo et al. 2001).

Fluvial-to-Estuarine Transition

The fluvial-to-estuarine transition appears in the Guadiana estuary as a high-amplitude, distinct reflector that is considered to represent the combined bay-line surface, sequence boundary (SB), and transgressive surface (TS) (Fig. 10) and is related to the absence of significant lowstand and early transgressive deposition (cf. Allen and Posamentier 1993, 1994; Nichol et al. 1996).

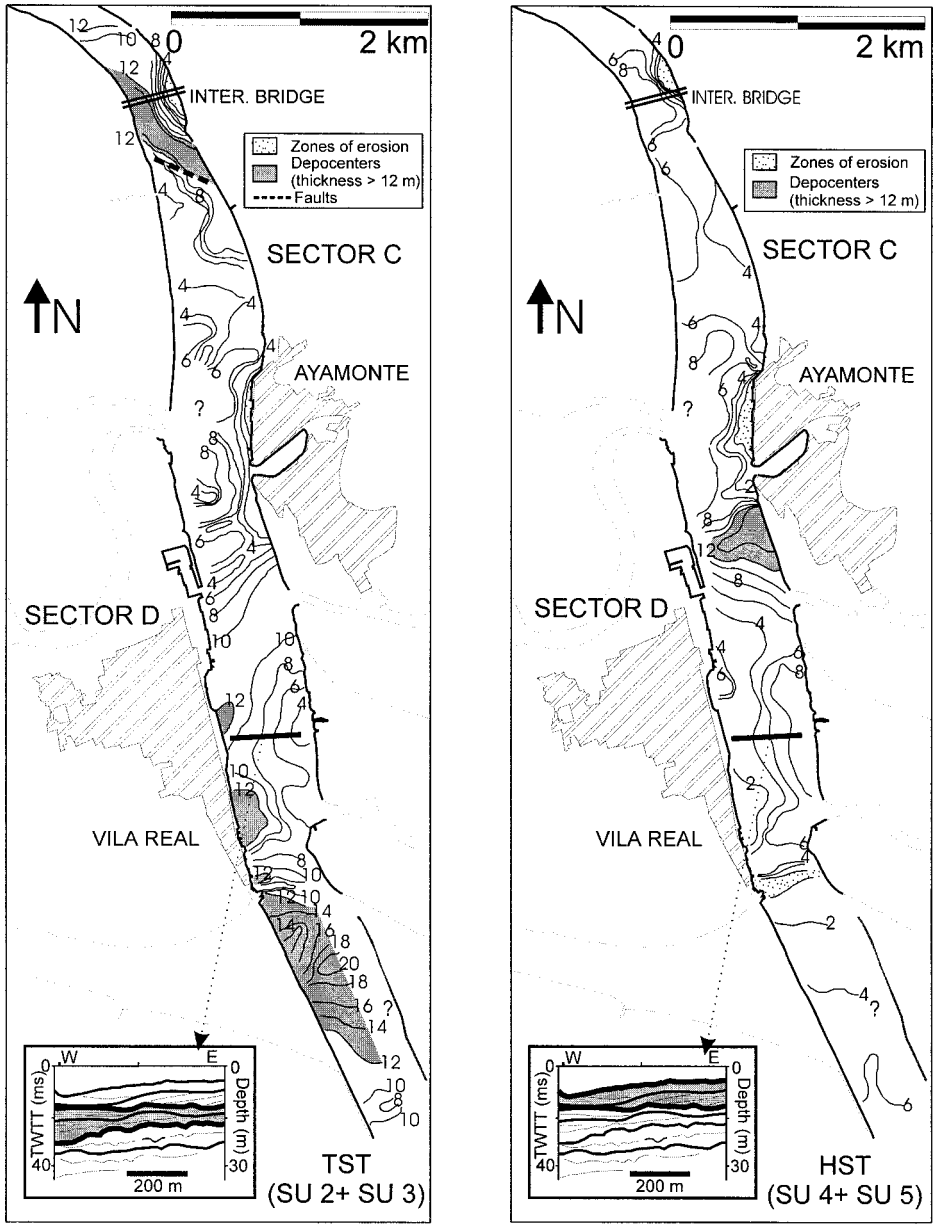

FIG. 11.—Distribution maps of the Holocene TST and HST, southward of the International Bridge (thickness values in meters).

Transgressive Deposits, Tidal Ravinement Surface (TRS), and Landward Incursion of Estuary-Mouth Sands

The Holocene estuarine fill of the Guadiana estuary is dominated by transgressive rather than highstand deposits. Transgressive deposits are usually over 10 m thick, particularly near the river mouth (Fig. 11). Several factors account for this dominance, including: (1) the influence of neotectonics, generating medium-scale depressions where transgressive deposits preferentially accumulated beyond effective tidal ravinement, as documented in other estuarine fills (Nichol et al. 1996); (2) limited influence of wave action and shoreface erosion inside the estuary, resulting in the significant preservation of the marine sand body (Dalrymple et al. 1992, 1994).

The TRS is easily recognized, because it overlies semitransparent deposits. It has a highly irregular pattern associated with significant tidal-channel incision developed during the final part of the postglacial transgression (Dalrymple and Zaitlin 1994). This surface should not be confused with a sequence boundary, because: (1) laterally it becomes a widespread, planar erosion surface where tidal influence is less pronounced and (2) it is not as distinct and high-amplitude as the sequence boundary.

The results suggest flood dominance during the transgressive period. Tidal erosion processes seem to have been dominant in the outer parts of the estuary, whereas flood-dominated currents were intensified around basement elevations, causing erosional depressions and landward introduction of coarse sediments. The strengthening of flood-related currents is related to maximum estuarine flooding. To explain the presence of relatively coarse material in inner estuarine zones, it is necessary to consider more efficient flood tidal activity or high coastal progradation rates during the highstand (Lessa et al. 1998), which probably occurred because of the progressive accretion of swash bars to construct prograding sand spit-tidal marsh complexes (Morales 1997).

Maximum Flooding Surface (MFS) and Highstand Deposits

The MFS is usually not easily recognized, because it can separate lithologically similar deposits (Allen and Posamentier 1993). In addition, the

downlap surface is substituted by inward-directed progradation where no bay-head delta exists (Dalrymple and Zaitlin 1994). The MFS is easily recognized in the Guadiana estuarine record, because it is marked by a change from flood to ebb dominance, especially in the outer estuary, where tidal-bar and distal-delta facies downlap onto this surface.

No evidence exists for a significant wave ravinement surface (WRS) in the Guadiana incised valley, which could indicate shoreface processes of low efficiency (Dalrymple and Zaitlin 1994). Its narrowness and the absence of a funnel morphology probably protected the inner estuarine valley, preventing significant wave erosion during maximum estuarine flooding.

Highstand deposits are usually thinner than 8 m and only locally thicker, infilling basement depressions (Fig. 11). Despite their moderate thickness, the widespread occurrence of highstand deposits in this estuary can be associated with the narrowness of the valley, because a broad distribution is expected to occur in small estuaries (Lessa et al. 1998). Similarly to what Fenster and FitzGerald (1996) observed in other areas, in the Guadiana estuary highstand deposition smoothes the bottom topography generated during the transgressive interval by enhanced tidal flows.

The thickness of Holocene deposits may reach more than 20 m in the littoral inner shelf adjacent to the Guadiana estuary (Morales 1993). If most of the transgressive deposits accumulated in the inner estuarine sections, it can be assumed that the bulk of those Holocene deposits in front of the estuarine valley constitute the HST. The higher development of the Holocene HST in front of the river mouth in relation with its moderate thickness in the estuarine valley can be explained by the conjunction of several factors, e.g., narrow valley morphology, increased fluvial supplies, and associated ebb dominance, which led to increased sediment export from the estuarine valley. As a consequence, two prodeltaic protuberances, evidenced in the bathymetric chart (Fig. 4) and possibly representing the two highstand progradational episodes, were generated. Further progradation of the highstand prodeltaic wedge might have been prevented by dominant oceanographic agents and by continuous export of the finest fraction to the shelf. This process would have led to the construction of a mid-shelf to outer-shelf depocenter during the whole highstand period, migrating southeastwards under the influence of shelf hydrodynamics (Nelson et al. 1999).

CONCLUSIONS

The sedimentary infilling of the Guadiana estuarine valley is complex, with five fifth order depositional sequences. It appears that the lower four sequences mainly constitute HSTs, inasmuch as they have the higher preservation potential in these protected environments. Conversely, the most recent sequence is composed of TST and HST deposits. The TST records the upper part of the postglacial transgression. The internal HST structure was determined by two small-amplitude sea-level cycles. Progradation occurred during stabilization periods and/or minor sea-level falls, whereas the transition was determined by a sea-level rise that probably led to delta lobe switching.

The influence of the estuary bedrock-controlled morphology on the hydrodynamic regime is particularly remarkable. The narrowness of the fluvial valley and moderate fluvial supply resulted in poor representation of Last Glacial Maximum lowstand deposits. Sediment export was reduced during the initial estuarine flooding, as depressions created by pre-Holocene neotectonic activity were preferred sites of transgressive accumulation. The continued transgression led to enhancement of flood currents around basement highs. This favored introduction of coarse sediments in more protected upstream zones. In contrast, estuarine geomorphology prevented a significant wave influence. During the highstand period, the narrow morphology of the estuary caused increased sediment bypass along the estuarine valley, leading to a widespread, moderate distribution of the HST in the estuarine channel and to the construction of a submarine prodeltaic wedge in front of the estuary mouth.

The main stratigraphic surfaces inside the estuarine fill are characterized by distinct seismic attributes. The most readily identifiable surface is the Würmian sequence boundary (SB), represented by a high-amplitude reflector evidencing a significant facies transition. The tidal ravinement surface (TRS) is characterized by strong ravinement and tidal-channel formation in the outer estuarine zones. The maximum flooding surface (MFS) is identified by change of stratal patterns and by progradation of tidal bars and prodelta deposits over transgressive estuary-mouth sands.

ACKNOWLEDGMENTS

This work was completed under the framework of the project ''ODIANA-EMERGE.'' The first author was funded by a Post-Doctoral FCT Portuguese Research Grant (Reference SFRH/BPD/5616/2001) and by a Marie Curie Individual Fellowship (contract nº HPMF-CT-2001-01494) between the Universidade de Algarve and The European Comission. The Wadiana 2000 survey was jointly organized by the Universidade do Algarve and the Instituto Español de Oceanografía. The participation of Francisco González, Lola Godoy, Marga García and Jorge Miranda is particularly acknowledged. Delminda Moura and Tomasz Boski (Universidade do Algarve, Portugal) made useful suggestions to improve the correlation between seismic profiles and estuary margin stratigraphy. Special thanks are due to Dr. Donatella Mellere (Exxon Mobil Upstream Research Company) and to Dr. Mary J. Kraus (JSR Editor), for their extensive and helpful revisions, which have significantly improved the manuscript. Brad Morris (Universidade do Algarve, Portugal) reviewed the English style of the manuscript. Sandra Fachin provided the Guadiana estuary map. Finally, the valuable help of the crew of the Esmeralda Azul is acknowledged.

REFERENCES

Allen, G.P., 1991, Sedimentary processes and facies in the Gironde estuary: a recent model for macrotidal estuarine systems, *in* Smith, D.G., Reinson, G.E., Zaitlin, B.A., and Rahmani, R.A., eds., Clastic Tidal Sedimentology: Canadian Society of Petroleum Geologists, Memoir 16, p. 29–40.

Allen, G.P., and Posamentier, H.W., 1993, Sequence stratigraphy and facies model of an incised valley fill: the Gironde estuary, France: Journal of Sedimentary Petrology, v. 63, p. 378–391.

Allen, G.P., and Posamentier, H.W., 1994, Transgressive facies and sequence architecture in mixed tide- and wave-dominated incised valleys: example from the Gironde estuary, France, *in* Dalrymple, R., Boyd, R., and Zaitlin, B.A., eds., Incised-Valley Systems: Origin and Sedimentary Sequences: SEPM, Special Publication 51, p. 225–239.

Allen, J.R.L., 1990, The Severn Estuary in southwest Britain: its retreat under marine transgression, and fine-sediment regime: Sedimentary Geology, v. 66, p. 13–28.

Bard, E., Hamelin, B., and Fairbanks, R.G., 1990, U–Th ages obtained by mass spectometry in corals from Barbados: sea level during the past 130,000 years: Nature, v. 346, p. 456–458.

Berger, A.L., 1992, Astronomical theory of paleoclimates and the last glacial–interglacial cycle: Quaternary Science Reviews, v. 11, p. 571–581.

Borrego, J., Morales, J.A., and Pendón, J.G., 1993, Holocene filling of an estuarine lagoon along the mesotidal coast of Huelva: The Piedras River mouth, southwestern Spain: Journal of Coastal Research, v. 9, p. 242–254.

Borrego, J., Morales, J.A., and Pendón, J.G., 1995, Holocene estuarine facies along the mesotidal coast of Huelva, south-western Spain, *in* Flemming, B.W., and Bartoloma, A., eds., Tidal Signatures in Modern and Ancient Sediments: International Association of Sedimentologists, Special Publication 24, p. 151–170.

Boski, T., Moura, D., Veiga-Pires, C., Camacho, S., Duarte, D., Scott, D.B., and Fernandes, S.G., 2002, Postglacial sea-level rise and sedimentary response in the Guadiana Estuary, Portugal/Spain border: Sedimentary Geology, v. 150, p. 103–122.

Boyd, R., and Honig, C., 1992, Estuarine sedimentation on the eastern shore of Nova Scotia: Journal of Sedimentary Petrology, v. 62, p. 569–583.

Brown, L.F., Jr., and Fisher, W.L., 1985, Seismic and stratigraphic interpretation and petroleum exploration: American Asociation of Petroleum Geologists, Continuing Education Course Note Series 16, 181 p.

Cearreta, A., 1994, Análisis micropaleontológico e interpretación paleoecológica del relleno sedimentario holoceno en el estuario del Bidasoa (Golfo de Bizkaia): Geobios, v. 27, p. 271–283.

Clavé, B., and Massé, L., in press, The ''Cordon de Richard'': morphology and internal structures of a 2,500 year-old Chenier-type ridge in the Gironde estuary area (SW France): Quaternary International.

Cooper, J.A.G., 1993, Sedimentation in a river dominated estuary: Sedimentology, v. 40, p. 979–1017.

Costa, C., 1994, Wind Wave Climatology of the Portuguese Coast: Final Report of Subproject A, NATO PO-WAVES Report 6/94-A, 80 p.

Chiocci, F.L., Ercilla, G., and Torres, J., 1997, Stratal architecture of Western Mediterranean Margins as the result of the stacking of Quaternary lowstand deposits below 'glacio-eustatic fluctuation base-level': Sedimentary Geology, v. 112, p. 195–217.

Dabrio, C.J., Zazo, C., Goy, J.L., Sierro, F.J., Borja, F., Lario, J., González, J.A., and Flores,

J.A., 2000, Depositional history of estuarine infill during the last postglacial transgression (Gulf of Cadiz, Southern Spain): Marine Geology, v. 162, p. 381–404.

Dalrymple, R.W., and Zaitlin, B.A., 1994, High-resolution sequence stratigraphy of a complex, incised valley succession, Cobequid Bay–Salmon River estuary, Bay of Fundy, Canada: Sedimentology, v. 41, p. 1069–1091.

Dalrymple, R.W., Boyd, R., and Zaitlin, B.A., 1994, History of research, types and internal organization of incised-valley systems: introduction to the volume, *in* Dalrymple, R.W., Boyd, R., and Zaitlin, B.A., eds., Incised-Valley Systems: Origin and Sedimentary Sequences: SEPM, Special Publication 51, p. 3–10.

Dalrymple, R.W., Zaitlin, B.A., and Boyd, R., 1992, Estuarine facies models: conceptual basis and stratigraphic implications: Journal of Sedimentary Petrology, v. 62, p. 1130–1146.

Dias, J.A., Boski, T., Rodrigues, A., and Magalhães, F., 2000, Coast line evolution in Portugal since the last glacial maximum until present—a synthesis: Marine Geology, v. 170, p. 177–186.

Esker, D., Eberli, G.P., and McNeill, D.F., 1998, The structural and sedimentological controls on the reoccupation of Quaternary incised valleys, Belize Southern Lagoon: American Association of Petroleum Geologists Bulletin, v. 82, p. 2075–2109.

Fenster, M.S., and FitzGerald, D.M., 1996, Morphodynamics, stratigraphy, and sediment transport patterns of the Kennebec River estuary, Maine, USA: Sedimentary Geology, v. 107, p. 99–120.

Frey, R.W., and Howard, J.D., 1986, Mesotidal estuarine sequences: a perspective from the Georgia Bight: Journal of Sedimentary Petrology, v. 56, p. 911–924.

García-Gil, S., Vilas, F., Muñoz, A., Acosta, J., and Uchupi, E., 1999, Quaternary Sedimentation in the Ría de Pontevedra (Galicia), Northwest Spain: Journal of Coastal Reseach, v. 15, p. 1083–1090.

González, R., Dias, J.M.A., and Ferreira, O., 2001, Study of a rapidly changing coastline using GIS: Recent evolution of the Guadiana Estuary (Southwestern Iberian Peninsula): Journal of Coastal Research, v. 34, p. 516–527.

Goy, J.L., Zazo, C., Dabrio, C.J., Lario, J., Borja, F., Sierro, F.J., and Flores, J.A., 1996, Global and regional factors controlling changes of coastlines in southern Iberia (Spain) during the Holocene: Quaternary Science Reviews, v. 15, p. 773–780.

Hernández-Molina, F.J., Somoza, L., and Lobo, F.J., 2000, Seismic stratigraphy of the Gulf of Cádiz continental shelf: a model for late Quaternary very high-resolution sequence stratigraphy and response to sea-level fall, *in* Hunt, D., and Gawthorpe, R.L.G., eds., Sedimentary Responses to Forced Regressions: Geological Society of London, Special Publication 172, p. 329–361.

Hernández-Molina F.J., Somoza, L., Rey, J., and Pomar, L., 1994, Late Pleistocene–Holocene sediments on the Spanish continental shelves: Model for very high resolution sequence stratigraphy: Marine Geology, v. 120, p. 129–174.

Hori K., Saito, Y., Zhao, Q., Cheng, X., Wang, P., Sato, Y., and Li, C., 2001, Sedimentary facies of the tide-dominated paleo-Changjiang (Yangtze) estuary during the last transgression: Marine Geology, v. 177, p. 331–351.

Instituto Hidrográfico, 1998, Tabela de Marés: volume I.

Larcombe, P., and Jago, C.F., 1994, The Late Devensian and Holocene evolution of Barmouth Bay, Wales: Sedimentary Geology, v. 89, p. 163–180.

Lericolais, G., Berné, S., and Féniès, H., 2001, Seaward pinching out and internal stratigraphy of the Gironde incised valley on the shelf (Bay of Biscay): Marine Geology, v. 175, p. 183–197.

Lessa, G.C., Meyers, S.R., and Marone, E., 1998, Holocene stratigraphy in the Paranaguá Bay estuary, southern Brazil: Journal of Sedimentary Research, v. 68, p. 1060–1076.

Lobo, F.J., 2000, Estratigrafía de alta resolución y cambios del nivel del mar durante el Cuaternario del margen continental del Golfo de Cádiz (S de España) y del Roussillon (S de Francia): estudio comparativo [unpublished PhD thesis]: University of Cádiz, Puerto Real, Spain, 618 p.

Lobo, F.J., Hernández-Molina, F.J., Somoza, L., and Díaz del Río, V., 2001, The sedimentary record of the post-glacial transgression on the Gulf of Cadiz continental shelf (Southwest Spain): Marine Geology, v. 178, p. 171–195.

Lobo, F.J., Hernández-Molina, F.J., Somoza, L., Díaz del Río, V., and Dias, J.M.A., 2002, Stratigraphic evidence of an upper Pleistocene TST to HST complex on the Gulf of Cádiz continental shelf (south-west Iberian Peninsula): Geo-Marine Letters, v. 22, p. 95–107.

Massé, L., Clavé, B., Tastet, J.-P., Diot, M.-F., and Lesueur, P., 2000, Chronology of the Holocene infill of the Gironde periestuarine marshes (SW France). Océanographie du golfe de Gascogne: VIIe colloque international, Biarritz, 4–6 April 2000, p. 236–241.

Morales, J.A., 1993, Sedimentología del estuario del Guadiana (S.W. España–Portugal) [Ph D thesis, published by the Publication Service of the University of Huelva, 1995]: University of Sevilla, Sevilla, Spain, 274 p.

Morales, J.A., 1995, Modelo de interacción de las corrientes de marea en la desembocadura del estuario mesomareal del Río Guadiana (S.O. España–Portugal): Geogaceta, v. 18, p. 83–86.

Morales, J.A., 1997, Evolution and facies architecture of the mesotidal Guadiana River delta (S.W. Spain–Portugal): Marine Geology, v. 138, p. 127–148.

Nelson, C.H., Baraza, J., Maldonado, A., Rodero, J., Escutia, C., and Barber, J.H., Jr., 1999, Influence of the Atlantic inflow and Mediterranean outflow currents on late Quaternary sedimentary facies of the Gulf of Cadiz continental margin: Marine Geology, v. 155, p. 99–129.

Nichol, S.L., Boyd, R., and Penland, S., 1996, Sequence stratigraphy of a coastal-plain incised valley estuary: Lake Calcasieu, Louisiana: Journal of Sedimentary Research, v. 66, p. 847–857.

Pascual, A., Weber, O., Rodríguez-Lazaro, J., Jouanneau, J.M., and Pujol, M., 1998, Le comblement de la ria de Gernika (golfe de Gascogne) à l'Holocène terminal: Oceanologica Acta, v. 21, p. 263–269.

Reynaud, J.-Y., Tessier, B., Proust, J.-N., Dalrymple, R., Bourillet, J.-F., de Batist, M., Lericolais, G., Berné, S., and Marsset, T., 1999, Architecture and sequence stratigraphy of a Late Neogene incised valley at the shelf margin, southern Celtic Sea: Journal of Sedimentary Research, v. 69, p. 351–364.

Rodríguez Ramírez, A., Rodríguez Vidal, J., Cáceres, L., Clemente, L., Belluomini, G., Manfra, L., Improta, S., and De Andrés, J.R., 1996, Recent coastal evolution of the Doñana National Park (SW Spain): Quaternary Science Reviews, v. 15, p. 803–809.

Saito, Y., 1995, High-resolution sequence stratigraphy of an incised-valley fill in a wave- and fluvial-dominated setting: latest Pleistocene–Holocene examples from the Kanto Plain of central Japan: Geological Society of Japan, Memoirs, v. 45, p. 76–100.

Shackleton, N.J., 1987, Oxygen isotopes, ice volume and sea level: Quaternary Science Reviews, v. 6, p. 183–190.

Somoza, L., Barnolas, A., Arasa, A., Maestro, A., Rees, J.G., and Hernández-Molina, F.J., 1998, Architectural stacking patterns of the Ebro delta controlled by Holocene high-frequency eustatic fluctuations, delta-lobe switching and subsidence processes: Sedimentary Geology, v. 117, p. 11–32.

Somoza, L., Hernández-Molina, F.J., De Andrés, J.R., and Rey, J., 1997, Continental shelf architecture and sea-level cycles: Late Quaternary high-resolution stratigraphy of the Gulf of Cádiz, Spain: Geo-Marine Letters, v. 17, p. 133–139.

Spanish Geological Survey, 1983, Mapa Geológico de España 1:50.000, Ayamonte, 39 p.

Thomas, M.A., and Anderson, J.B., 1994, Sea-level controls on the facies architecture of the Trinity/Sabine incised-valley systems, Texas continental shelf, *in* Dalrymple, R.W., Boyd, R., and Zaitlin, B.A., eds., Incised-Valley Systems: Origin and Sedimentary Sequences: SEPM, Special Publication 51, p. 63–82.

Woodroffe, C.D., Chappell, J., Thom, B.G., and Wallensky, E., 1989, Depositional model of a macrotidal estuary and floodplain, South Alligator River, Northern Australia: Sedimentology, v. 36, p. 737–756.

Zazo, C., Dabrio, C.J., Borja, F., Goy, J.L., Lezine, A.M., Lario, J., Polo, M.D., Hoyos, M., and Boersma, J.R., 1999, Pleistocene and Holocene aeolian facies along the Huelva coast (southern Spain): climatic and neotectonic implications: Geologie en Mijnbouw, v. 77, p. 209–224.

Zazo, C., Goy, J.L., Lario, J., and Silva, P.G., 1996, Littoral zone and rapid climate changes during the last 20 000 years. The Iberian study case: Zeitschrift für Geomorphologie, v. 102, p. 119–134.

Zazo, C., Goy, J.L., Somoza, L., Dabrio, C.J., Belluomini, G., Improta, S., Lario, J., Bardají, T., and Silva, P.G., 1994, Holocene sequence of sea-level fluctuations in relation to climatic trends in the Atlantic–Mediterranean linkage coast: Journal of Coastal Research, v. 10, p. 933–945.

Zhang, G., and Li, C., 1996, The fills and stratigraphic sequences in the Qiantangjiang incised paleovalley, China: Journal of Sedimentary Research, v. 66, p. 406–414.

Received 3 January 2002; accepted 23 March 2003.